PHYSICAL REVIEW B VOLUME 53, NUMBER 22 1 JUNE 1996-II

Rare-earth ion size effect on resistivity, susceptibility, and superconductivity of $R\mathrm{Ba_2Cu_{3-x}Zn_xO_{7-y}}$ ($R=$ Yb, Er, Y, Dy, Gd, Eu, Sm, and Nd)

Yunhui Xu,* S. S. Ata-Allah,† M. G. Berger, and O. Glück
Institut für Schicht- und Ionentechnik, Forschungszentrum Jülich Gesellschaft mit beschränkter Haftung,
Postfach 1913, D-52425 Jülich, Germany

(Received 5 June 1995; revised manuscript received 27 November 1995)

A systematic study of Zn doping on the resistivity ρ, dc susceptibility χ, and superconducting T_c of $R\mathrm{Ba_2Cu_{3-x}Zn_xO_{7-y}}$ systems (R=Yb, Er Y, Dy, Gd, Eu, Sm, and Nd, and $0 \leqslant x \leqslant 0.3$) is reported. X-ray powder diffraction (XRD) shows that all samples consist essentially of a single phase and retain the orthorhombic structure in the range of $0 \leqslant x \leqslant 0.3$ (except for R=Yb in the range of $0 \leqslant x \leqslant 0.15$). By analyzing our Raman spectra and XRD data, Zn atoms are found more likely to substitute on Cu(2) sites. Doping with Zn on the Cu site in these systems causes a rapid nearly linear decrease of T_c as Zn content increases. The reduction of T_c for $R\mathrm{Ba_2Cu_{3-x}Zn_xO_{7-y}}$ is found to depend strongly on the ionic radius of the rare-earth element R. This effect resembles the ion size effect on T_c in $R_{1-x}\mathrm{Pr}_x\mathrm{Ba_2Cu_3O_{7-y}}$, where Pr substitutes on the R site, and in $R\mathrm{Ba_2Cu_{3-x}Ga_xO_{7-y}}$, where Ga substitutes on the Cu(1) sites in Cu-O chains, although in the $R\mathrm{Ba_2Cu_{3-x}Zn_xO_{7-y}}$ systems Zn is found to be more likely to substitute on the Cu(2) sites in Cu-$\mathrm{O_2}$ planes. The suppression of superconductivity by zinc and the rare-earth ion size effect on T_c in these systems is interpreted in terms of a Mott spin bipolaron model. [S0163-1829(96)04722-4]

INTRODUCTION

Substitution with rare-earth elements on the Y site and with transition or sp elements on the Cu site of the high-T_c superconductor (HTSC) $\mathrm{YBa_2Cu_3O_{7-y}}$ is an important method for understanding the mechanism of the occurrence of superconductivity at high temperatures. Of special interest for clarifying the effect of impurities on the superconductivity and various characteristics of the HTSC is the substitution for copper by metals such as Ti, V, Cr, Mn, Fe, Co, Ni, Zn, Ga, and Al.[1–43] The research on the respective importance of the two copper sites in $\mathrm{YBa_2Cu_3O_{7-y}}$, Cu(1) in the CuO chains and Cu(2) in the $\mathrm{CuO_2}$ planes, for the superconductivity has been reported in great detail. Most groups found that nominally trivalent elements [like Ga,[1–3,7–10] Fe,[1–5,8,10,21,27] Co,[1–4,8,10,14–16,18,21,27] and Al (Refs. 3,4,8 and 10)] substitute on Cu(1) sites and cause a moderate reduction in T_c, while nominally divalent dopants [like Zn (Refs. 1,4–6,8,10,18,20–22 and 28) and Ni (Refs. 1–4,8,10,11,14 and 15)] primarily occupy the Cu(2) sites and suppress T_c drastically. The largest rate of reduction of T_c was ~13 K/% atom for Zn substitution on the plane site[1,8] and 5 K/% atom for Co substitution on the chain site.[4,8] These results show that the Cu(2)-O planes play a more important role than the Cu(1)-O chains in the 123 superconductors.[1,6,11,12,14,15]

With considerable interest in the drastic suppression of T_c, numerous studies on the substitution for Cu in $\mathrm{YBa_2Cu_3O_{7-y}}$, with nonmagnetic Zn having a definite valence state 2+ and filled $3d$ levels, have been carried out.[1–43] Some consistent results were obtained: (1) the solution limits is 9–10 %,[4,11,16,17,19,20,29] (2) the orthorhombic structure is retained,[1–43] (3) the oxygen content is little affected by 10% Zn doping ($7-y \geqslant 6.9$),[4,11–13,17,23,25] and (4) the rate of T_c reduction is 8–15 K/%, the largest known to date.[1,8,19,39] The site occupancies of Zn atoms have been investigated by using neutron diffraction,[1,5,6,23,24] Raman spectra,[18] extended x-ray-absorption fine-structure analysis,[6] x-ray absorption near-edge studies,[21] nuclear magnetic resonance,[9,10,20,29] nuclear quadrupole resonance,[22] thermogravimetric analysis,[4] and some other methods;[25–28] however, the results of site occupation probabilities of Zn are controversial. Most research groups find that zinc preferential occupies the Cu(2) sites in Cu-$\mathrm{O_2}$ planes in accord with our observations,[1,4–6,8,10,18,20–22,28,29,31,34] although some groups claimed the substitution of Zn for both the Cu(1) and Cu(2) sites.[9,15,23–27]

For the Pr-substituted 123 compounds (on the R sites), $R_{1-x}\mathrm{Pr}_x\mathrm{Ba_2Cu_3O_{7-y}}$ (R=Lu, Yb, Tm, Er, Ho, Y, Dy, Gd, Eu, Sm, and Nd, and $0 \leqslant x \leqslant 1$), it was established that the superconducting transition temperature T_c decreases monotonically with increasing Pr concentration x, and, at a constant Pr concentration, T_c decreases approximately linearly with increasing radius of the R ions.[44–46] The magnetic ordering temperature T_N of Pr ions in $R_{1-x}\mathrm{Pr}_x\mathrm{Ba_2Cu_3O_{7-y}}$ systems (R=Yb, Tm, Er, Y, Ho, Dy, Gd, Eu, Sm, and Nd) with $x=0.5$–1.0 was observed to decrease monotonically with increasing R concentration $(1-x)$; and at a constant x, T_N is R ion size dependent.[45,46] These results were interpreted qualitatively in terms of the hybridization between the local states of the Pr ion and the valence-band states of the $\mathrm{CuO_2}$ planes.[44–46]

This rare-earth ion size effect is also found in Ga-doped [on Cu(1) sites] $R\mathrm{Ba_2Cu_{3-x}Ga_xO_{7-y}}$ systems.[47,48] It was observed that for $R\mathrm{Ba_2Cu_{3-x}Ga_xO_{7-y}}$ systems[47,48] (where R=Yb, Er, Y, Dy, Gd, Eu, and Nd, at $x=0$, 0.05, 0.1, 0.15, 0.2, and 0.3), the melting point, the critical Ga concentration x_{O-T} (at which the samples undergo a phase transition from orthorhombic to tetragonal), the normal state resistivity ρ_n, and the superconducting T_c are dependent upon the rare-earth ion size. It was suggested that a decrease in the density of states $N(E_F)$ or localization of carriers due to Ga substitution are the possible mechanisms for suppression of super-

0163-1829/96/53(22)/15245(9)/$10.00

conductivity. The Mott transition was used for interpreting the superconducting-nonsuperconducting transition accompanied by a transition into the semiconducting phase in these systems.[47,48]

Since most groups observed that Zn substitutes on the Cu(2) sites in 123 systems, it is very interesting to study the effect of Zn doping on the properties of different rare-earth 123 compounds. In this paper we present a detailed investigation of the structural properties, resistivity ρ, dc susceptibility χ, and superconductivity of the Zn-substituted $R\mathrm{Ba}_2\mathrm{Cu}_{3-x}\mathrm{Zn}_x\mathrm{O}_{7-y}$ systems (R=Yb, Er, Y, Dy, Gd, Eu, Sm, and Nd) with $0 \leqslant x \leqslant 0.3$.

EXPERIMENT

Polycrystalline $R\mathrm{Ba}_2\mathrm{Cu}_{3-x}\mathrm{Zn}_x\mathrm{O}_{7-y}$ (R=Yb, Er, Y, Dy, Gd, Eu, Sm, and Nd) with $0 \leqslant x \leqslant 0.3$ samples were prepared by the solid-state reaction method. Stoichiometric powders of $R_2\mathrm{O}_3$, BaCO_3, CuO, and ZnO with a purity $\geqslant$99.99% were thoroughly mixed in an agate mortar, and calcined at 915 °C for 24 h. The resultant powders were reground and refired to improve the homogeneity. After a final careful grinding these powders were pressed with 4 kbar into $5\times30\times1\text{-mm}^3$ rectangular bars. These bars were sintered in oxygen flow at 925–930 °C (except R=Yb at 920 °C) for 72 h followed by additional annealing at 680°C for 10 h and 400 °C for 10 h. Finally these bars were furnace cooled in oxygen flow to room temperature over about 10 h. Powder x-ray-diffraction (XRD) studies at room temperature using a Stoe Automatic Diffractometer with Co $K\alpha$ radiation (λ=1.788970 Å) were carried out for all $R\mathrm{Ba}_2\mathrm{Cu}_{3-x}\mathrm{Zn}_x\mathrm{O}_{7-y}$ samples.

Raman spectra were taken for polycrystalline $\mathrm{YBa}_2\mathrm{Cu}_{3-x}\mathrm{Zm}_x\mathrm{O}_{7-y}$ with x=0, 0.04, 0.06, 0.1, 0.15, 0.2, and 0.3 using a DILOR XY triple monochromator which was equipped with a multichannel detection system. For excitation of the 514.5-nm line an argon-ion laser was used. To avoid heating effects the laser power used was 2 mW, and the spot diameter on the sample was 100 μm. The scattering geometry was $z(yy)z$ in Porto notation. The experimental error for the measurements is about $\pm0.3\ \mathrm{cm}^{-1}$. From each sample three spectra were recorded at different locations on the sample. The peak maxima were extracted by fitting a Lorentz line shape, and in addition were estimated by eye.

The normal-state resistivity and superconducting transition temperature T_c were measured by standard four-probe technique for regular bars on which Al-foil electrical leads were regularly arranged with silver paste epoxy. Magnetization was measured using a quantum design magnetometer at both zero-field cooling (ZFC) and field cooling (FC) in a magnetic field of 5 Oe.

RESULTS AND DISCUSSION

XRD patterns indicate that the compound of nominal composition with $0 \leqslant x \leqslant 0.3$ and R=Er, Y, Dy, Gd, Eu, Sm,

TABLE I. The lattice parameters a, b, and c of $R\mathrm{Ba}_2\mathrm{Cu}_{3-x}\mathrm{Zn}_x\mathrm{O}_{7-y}$ (R=Yb, Er, Y, Dy, Gd, Eu, Sm, and Nd) at various Zn concentration x. The last numbers of each a, b, and c were estimated.

	Lattice	Zn Content x							
Rare earth	parameters (Å)	0	0.01	0.02	0.04	0.06	0.08	0.1	0.15
Yb	a	3.8766	3.8687	3.8749	3.8807	3.8821	3.8787		
	b	3.8014	3.8009	3.8032	3.8084	3.8054	3.8094		
	c	11.6460	11.6558	11.6509	11.6557	11.6536	11.6598		
Er	a	3.8776	3.8787	3.8758	3.8757	3.8799	3.8763	3.8767	3.8793
	b	3.8094	3.8085	3.8055	3.8084	3.8093	3.8070	3.8075	3.8084
	c	11.6549	11.6592	11.6466	11.6525	11.6495	11.6501	11.6498	11.6586
Y	a	3.8860	3.8860	3.8877	3.8858	3.8860	3.8861	3.8859	3.8873
	b	3.8176	3.8178	3.8198	3.8172	3.8169	3.8172	3.8179	3.8182
	c	11.6688	11.6645	11.6651	11.6635	11.6635	11.6658	11.6673	11.6664
Dy	a	3.8945	3.8891	3.8953	3.8868	3.8865	3.8848	3.8869	3.8867
	b	3.8362	3.8258	3.8290	3.8212	3.8227	3.8215	3.8218	3.8290
	c	11.6840	11.6731	11.6724	11.6742	11.6773	11.6798	11.6756	11.6994
Gd	a	3.8979	3.9056	3.9076	3.9091	3.9076	3.9073	3.9095	3.9092
	b	3.8384	3.8422	3.8472	3.8438	3.8452	3.8467	3.8443	3.8469
	c	11.7026	11.7028	11.7156	11.7168	11.7218	11.7219	11.7218	11.7275
Eu	a	3.8975	3.8922	3.8983	3.8990	3.8996	3.9017	3.8962	3.8999
	b	3.8395	3.8345	3.8394	3.8394	3.8401	3.8427	3.8386	3.8400
	c	11.7090	11.7137	11.7179	11.7159	11.7165	11.7168	11.7174	11.7186
Sm	a	3.9028	3.9046	3.9060	3.9059	3.9066	3.9034	3.9089	3.9134
	b	3.8487	3.8494	3.848	3.8507	3.8498	3.8482	3.8534	3.8558
	c	11.7325	11.7367	11.7361	11.7334	11.7356	11.7373	11.7372	11.7354
Nd	a	3.9183	3.9125	3.9146	3.9166	3.9105	3.9147	3.9158	3.9174
	b	3.8608	3.8633	3.8604	3.8624	3.8602	3.8566	3.8586	3.8589
	c	11.7725	11.7741	11.7735	11.7786	11.7704	11.7884	11.7796	11.7725

and Nd have a single-phase orthorhombic perovskitelike $YBa_2Cu_3O_{7-y}$ structure with an impurity level of less than 5%, while the samples with $R=Yb$ have weak extra peaks corresponding to a few percent of foreign phase inclusion, which are increased for Zn concentration $x\geqslant 0.1$.

The lattice parameters were determined using a standard least-squares fit to the positions of at least 18 diffraction peaks. Table I lists the lattice parameters a, b, and c of $RBa_2Cu_{3-x}Zn_xO_{7-y}$ samples ($R=$Yb, Er, Y, Dy, Gd, Eu, Sm, and Nd) at Zn content $0\leqslant x\leqslant 0.15$. Detailed x-ray powder diffraction measurements show that the structure remains orthorhombic throughout the substitution range ($0\leqslant x\leqslant 0.3$). The lattice parameters a, b, and c are very close to those of undoped $RBa_2Cu_3O_{7-y}$ ($R=$Yb, Er, Y, Dy, Gd, Eu, Sm, and Nd). The orthorhombicity $(a-b)/(a+b)$ seems to be independent of the Zn concentration x in the range $0\leqslant x\leqslant 0.3$. This indicates that the oxygen vacancy order or the linear chain structures of the Cu(1)-O sites remains intact. Therefore it may be inferred that Zn replaces Cu in the planes adjacent to the R planes rather than in the Cu-O chains, thus retaining the orthorhombic structure.

Raman spectra of $YBa_2Cu_{3-x}Zn_xO_{7-y}$ samples have been measured for further identifying the site occupation of Zn atoms. Five A_g symmetry phonons in orthorhombic $YBa_2Cu_3O_{7-y}$ are found at about 502, 435, 340, 151, and 116 cm^{-1} that involve the vibration of Ba, Cu, or O atoms along the c axis.[49–51] The Raman frequency 500 cm^{-1} has been assigned to the in-phase vibration of the apex oxygen [O(4)], 430 and 340 cm^{-1} to the vibration of the plane oxygen [O(2)/O(3)] in phase and out of phase, respectively; and 150 cm^{-1} to the vibration of plane copper [Cu(2)] and 116 cm^{-1} to the vibration of barium.[49–51] The dependence of the Raman frequency on the Zn content x for the four modes (about 502, 435, 340, and 150 cm^{-1}) of $YBa_2Cu_{3-x}Zn_xO_{7-y}$ is illustrated in Fig. 1. Although the data are scattered within ± 2 cm^{-1} due to collection from various locations on the polycrystalline samples, some trends still can be seen. In Fig. 1 the 500-cm^{-1} Raman line [associated with the axial symmetric vibration of O(4) about the Cu(1) along the c axis] is not dependent on the replacement of Cu by Zn up to 10% substitution (Fig. 1), implying that there are not bond length changes between Cu(1)-O(4) and Cu(2)-O(4), especially no distortion in the chain. This suggests that Zn is not replaced on the Cu(1) sites. In contrast, the 500-cm^{-1} mode for M-substituted $YBa_2Cu_{3-x}M_xO_{7-y}$ where $M=$Co (Refs. 18, 52, and 53) or Fe,[18] and for Ga-substituted $PrBa_2Cu_{3-x}Ga_xO_{7-y}$ (Ref. 54) systems, shifts to lower frequency with increased doping, implying that Co, Fe, or Ga atoms replaced on the Cu(1) sites.[18,52–54] In Fig. 1 both the 430- and 340-cm^{-1} Raman lines shift to higher frequencies with increasing Zn content. The vibration of the plane oxygen is influenced due to the replacement of copper by zinc, therefore one can suppose that Zn atoms most likely reside in the plane Cu(2) sites. The 150-cm^{-1} Raman line shows a weak trend to lower frequency with increasing Zn concentration x, again indicating that the vibration of plane Cu is slightly affected. The trends of mode 500 and 430 cm^{-1} in Fig. 1 are in good agreement with the results of Roughani *et al.*[18] However, the behavior of modes 340 and 150 cm^{-1} in Fig. 1 was not reported in Ref. 18.

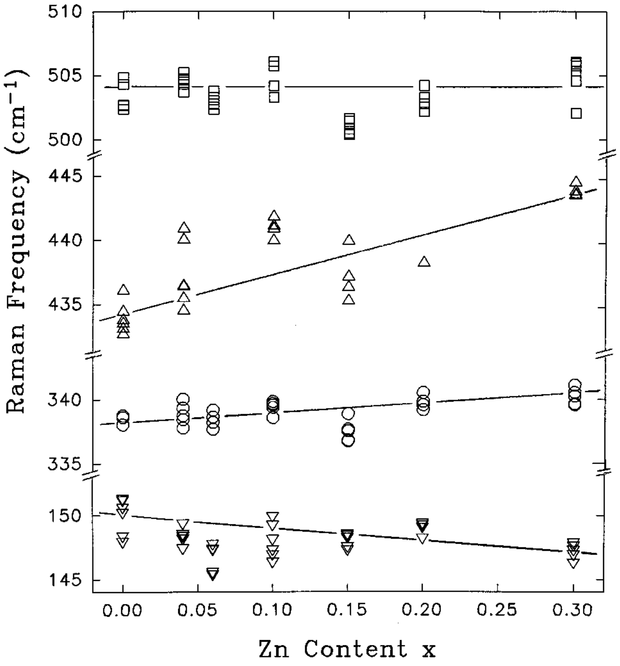

FIG. 1. Dependence of the Raman frequency on the Zn concentration x for $YBa_2Cu_{3-x}Zn_xO_{7-y}$. (The experimental error for the measurements is about ± 0.3 cm^{-1}.)

Figure 2 shows the temperature dependence of the electrical resistivity of $RBa_2Cu_{3-x}Zn_xO_{7-y}$ systems with Zn concentrations $x=0.01$ and 0.1. The decrease of T_c with increasing Zn substitution levels is clearly demonstrated. In Fig. 2 all the resistivity curves are shifted upwards with increasing x, implying that the primary effect of Zn scattering is to add a nominally temperature-independent contribution to the transport scattering rate. The samples of $R=$Yb, Er, Y, and Dy are metallic in the substitution range $0\leqslant x\leqslant 0.1$, with a positive temperature coefficient of resistivity (TCR). The average TCR for these systems increases as x increases in the range of $x\leqslant 0.1$ and $T>100$ K. This may be due to the localization of carriers, or an unsuspected temperature-dependent contribution by the Zn centers. For systems where $R=$Gd, Eu, Sm,and Nd in the vicinity of $x=0.06$ for Gd and Eu, and 0.02 for Sm and Nd, the variation of ρ with lowering temperature tends to become flat, with an increasing tendency at temperatures near T_c.

At higher substitution levels the normal-state resistivity presents a semiconducting character with a negative TCR, and causes a significant degradation in superconductivity. Figure 3 demonstrates the temperature dependence of the resistivity ρ of $RBa_2Cu_{3-x}Zn_xO_{7-y}$ with $x=0.3$. At the same concentration of Zn ($x=0.1$ or 0.3) the resistivity strongly depends on the different R ions. An obvious trend that the normal-state resistivity ρ increases with increasing ion size of R is seen in Figs. 2 and 3.

To compare the normal-state resistivity at the same Zn substitution level in different $RBa_2Cu_{3-x}Zn_xO_{7-y}$ systems, Table II lists the radius of R ions, and the data of resistivity ρ at 290, 200, and 100 K, with $x=0.02$, and 0.08, where all TCR's are positive (metallic behavior). At constant x, there

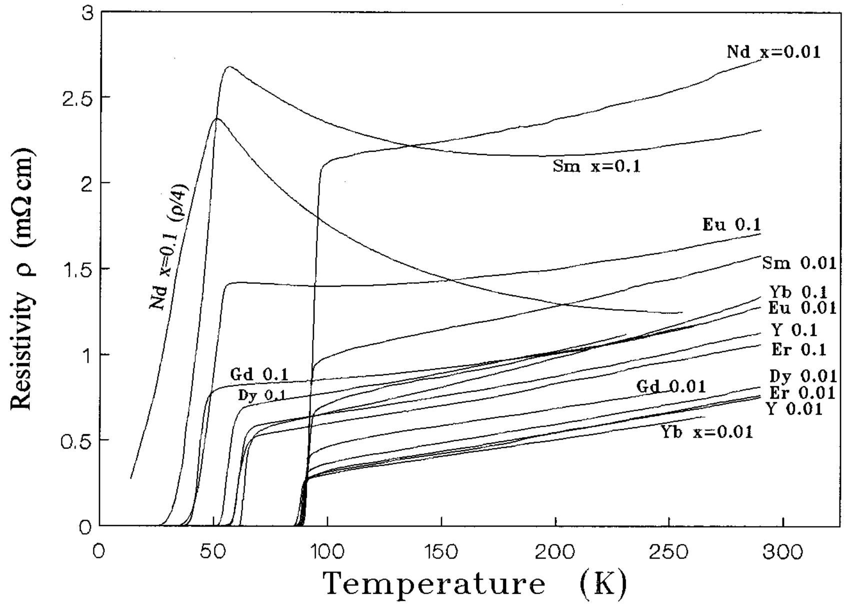

FIG. 2. Temperature dependence of resistivity ρ of RBa$_2$Cu$_{3-x}$Zn$_x$O$_{7-y}$ (R=Yb, Er, Y, Dy, Gd, Eu, Sm, and Nd) at Zn content $x=0.01$ and 0.1.

is a trend that the resistivity ρ increases with increasing ionic radius of R (except for R=Yb, where some additional scattering from impurity phases visible in XRD probably exists). This means that the carrier localization or the effect of Zn scattering is affected by the R plane.

In RBa$_2$Cu$_{3-x}$Zn$_x$O$_{7-y}$ systems for $x=0.3$ and R=Dy, Gd, Eu, Sm, and Nd, and for $x=0.2$, R=Sm and Nd, the samples were not superconducting down to 4.2 K, and showed only a semiconductorlike character. At low temperatures the results can be interpreted in terms of the Mott variable range hopping law (VRH), and follow a universal behavior, $\rho(T)=\rho_0 \exp(T/T_0)^{-1/4}$ (Ref. 55) [see Fig. 4(a)]. Near room temperature the resistivity can be fitted by an exponential function of $1/T$, $\rho(T)=\rho_3 \exp(E_3/kT)$ [see Fig. 4(b)], indicating that at high temperatures (~290 K) the contribution to the electrical conductivity comes from nearest-neighbor hopping (NNH).[56] Such hopping mechanism (VRH and NNH) for conductivity, which were also observed in PrBa$_2$Cu$_{3-x}$Ga$_x$O$_{7-y}$ (Ref. 57) and RBa$_2$Cu$_{3-x}$Ga$_x$O$_{7-y}$ (Ref. 47) systems, seem to be common features of insulating copper oxide 123 compounds. It should be noted, however, that the replacement of divalent Zn^{2+} for Cu^{2+} on the planes probably induces localization of mobile holes rather than hole filling. This differs from the effect of the replacement of trivalent Ga^{3+} for chain copper in PrBa$_2$Cu$_{3-x}$Ga$_x$O$_{7-y}$ (Ref. 57) and RBa$_2$Cu$_{3-x}$Ga$_x$O$_{7-y}$ (Ref. 47) systems, for which both the decrease of hole number by hole filling and hole localization were supposed. This could perhaps be a reason why Zn doping does not increase ρ remarkably in comparison with Ga doping in insulating 123 compounds.[47,57]

We have studied the dependence of $T_{c,\mathrm{mid}}$ (corresponding to the midpoint of the resistive superconducting transition curve) on the concentration of Zn for RBa$_2$Cu$_{3-x}$Zn$_x$O$_{7-y}$ (R=Yb, Er, Y, Dy, Gd, Eu, Sm, and Nd, and $0 \leqslant x \leqslant 0.3$). We have found that T_c decreases nearly linearly with increasing Zn substitution levels for all studied RBa$_2$Cu$_{3-x}$Zn$_x$O$_{7-y}$ systems. However, the rates of T_c

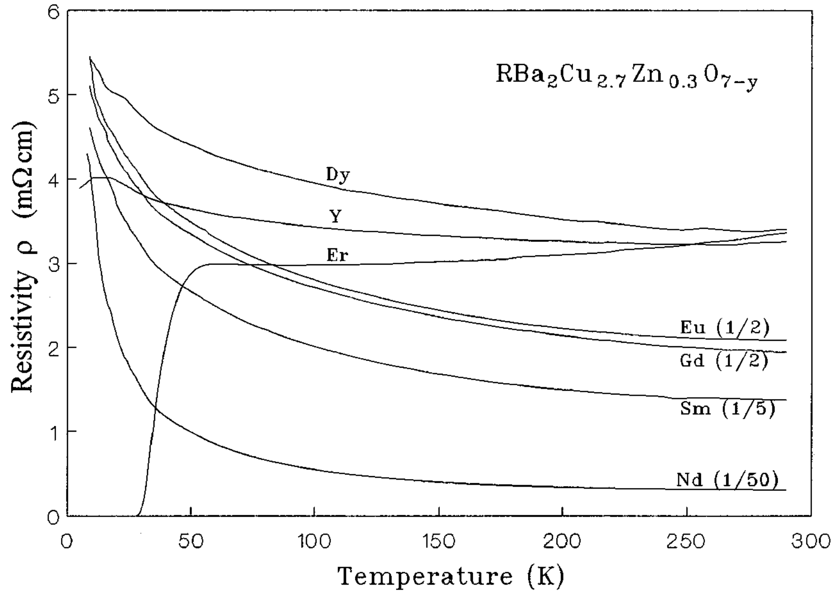

FIG. 3. Resistivity ρ vs temperature for RBa$_2$Cu$_{2.97}$Zn$_{0.3}$O$_{7-y}$ (R=Yb, Er, Y, Dy, Gd, Eu, Sm, and Nd).

TABLE II. The dependence of the normal-state resistivity ρ of $R\text{Ba}_2\text{Cu}_{3-x}\text{Zn}_x\text{O}_{7-y}$ at 290, 200, and 100 K, with Zn content $x=0.02$ and 0.08, where all the TCR's are positive (metallic behavior), on the ionic radius of the element R ($R=$Yb, Er, Y, Dy, Gd, Eu, Sm,and Nd). The superconducting transition temperature T_c is also present.

Zn content	Rare earth	Ionic radius	$T_{c,\text{ mid}}$	Resistivity	ρ (mΩ cm)	
x		(pm)	(K)	at 290 K	200 K	100 K
0.02	Yb	85.8	83.67	0.85	0.581	0.351
	Er	88.1	84.94	0.807	0.588	0.367
	Y	89.3	85.1	0.781	0.565	0.35
	Dy	90.8	85.07	0.887	0.661	0.435
	Gd	93.8	86.5	0.956	0.742	0.528
	Eu	95.0	86.64	1.355	1.088	0.797
	Sm	96.4	86.5	1.709	1.404	1.089
	Nd	99.5	86.14	4.464	3.911	3.899
0.08	Yb	85.8	70.92	1.284	0.927	0.608
	Er	88.1	62.19	0.983	0.745	0.522
	Y	89.3	61.82	1.06	0.814	0.589
	Dy	90.8	60.34	1.108	0.868	0.665
	Gd	93.8	55.11	1.224	0.957	0.791
	Eu	95.0	53.7	1.602	1.362	1.212
	Sm	96.4	51.8	1.860	1.629	1.597
	Nd	99.5	36			

suppression, dT_c/dx, are quite different in various systems with different R's. The experimental data of average $[dT/_c/d(x/3)]$ of $R\text{Ba}_2\text{Cu}_{3-x}\text{Zn}_x\text{O}_{7-y}$, deduced from the slopes of the $T_c(x)$ linear lines, are -7.8, -8.5, -8.7, -9.9, -11.3, -13.0, -13.7, and -23.9 K/at. %, for $R=$Yb, Er, Y, Dy, Gd, Eu, Sm, and Nd, respectively. The rates of T_c suppression in Zn-doped systems are larger than that in Ga-substituted systems (for example, $[dT_c/d(x/3)_{x=0}]$ are -1.9, -2.9, -6.0, -7.9, and -23.5 K/at. %, for $R\text{Ba}_2\text{Cu}_{3-x}\text{Ga}_x\text{O}_{7-y}$, $R=$Er, Y, Dy, Eu, and Nd, respectively[47]). The relative effectiveness of Zn in destroying superconductivity can be attributed in part to Zn substitution on the planar sites, where it is widely believed that the superconductivity resides.

The superconducting transition width ΔT_c, which is taken as the difference between $T_{c,\text{mid}}$ and $T_{c,\text{zero}}$ (the temperature at which the resistivity drops to zero), increases with increasing Zn concentration for each R, and also with increasing ionic radius of the rare-earth element when the Zn concentration is kept constant (Fig. 5). Loram, Mizra, and Freeman[30] discussed the transition width of the system $\text{YBa}_2\text{Cu}_{3-x}\text{Zn}_x\text{O}_{7-y}$ based on electronic specific-heat measurements. The sharp superconducting anomalies at T_c (for $x=0$ and 1% Zn doping) demonstrated that the superconducting order parameter at T_c was phase coherent over large volumes containing many pairs. For the 3% Zn-doped sample the increased rounding of the anomaly demonstrated limited phase coherence (a spread of T_c) when the mean separation of zinc ions fell below ~ 13 Å which is comparable with a mean coherence length.[30] However, this can not account for the effect of the ion size on ΔT_c shown in Fig. 5. For example, for 1.3% Zn-doped ($x=0.04$) samples, the width ΔT_c of $\text{NdBa}_2\text{Cu}_{2.96}\text{Zn}_{0.04}\text{O}_{7-y}$ is three times larger than that of $\text{YBa}_2\text{Cu}_{2.96}\text{Zn}_{0.04}\text{O}_{7-y}$, and the mean separation of Zn ions in the former ($R=$Nd) should be larger than that in the latter ($R=$Y), since the $R=$Nd compound has larger lattice parameters.

We have compared the dependence of $T_{c,\text{mid}}$ and the normal-state resistivity ρ at $T=290$ and 100 K of $R\text{Ba}_2\text{Cu}_{3-x}\text{Zn}_x\text{O}_{7-y}$ on the Zn concentration x. The values of the critical concentration x_{cr} required to suppress T_c to zero are estimated to be around 0.21, 0.19, 0.17, and 0.11 for $R=$Gd, Eu, Sm, and Nd, respectively. The rate of change of resistivity with x remarkably increases at the critical concentration x_{cr}, indicating that semiconductorlike behavior accompanies the destruction of the superconducting phase. These results indicate that variations of the Zn concentration influence the electronic states of the materials: the density of states, or the mobility of the charge carriers.

As an example for all systems discussed above, the temperature dependence of the dc susceptibility per mol χ for $\text{DyBa}_2\text{Cu}_{3-x}\text{Zn}_x\text{O}_{7-y}$ samples with $x=0$, 0.02, 0.04, 0.06, 0.08, and 0.1, at both zero-field cooling (ZFC) and field cooling (FC) is shown in Fig. 6. The transition temperatures $T_{c,\text{ mag}}$ evaluated by linearly extrapolating (near T_c) ZFC diamagnetic $M(T)$ curves to $M=0$ are well consistent with $T_{c,\text{mid}}$, deduced from resistivity measurements. Doping with Zn not only suppresses T_c, but also reduces the fractions of diamagnetic shielding, indicating the reduction in the fraction of superconducting materials or phase separation in samples with higher Zn content in spite of the fact that XRD measurements showed single-phase structures in these samples.

To compare the effect of the same amount of Zn doping on samples with various R, Fig. 7 plots the dc susceptibility per mol χ versus temperature of $R\text{Ba}_2\text{Cu}_{2.9}\text{Zn}_{0.1}\text{O}_{7-y}$ at ZFC for $R=$Yb, Er, Dy, EU, Sm, and Nd. Figure 7 demonstrates that at a constant Zn concen-

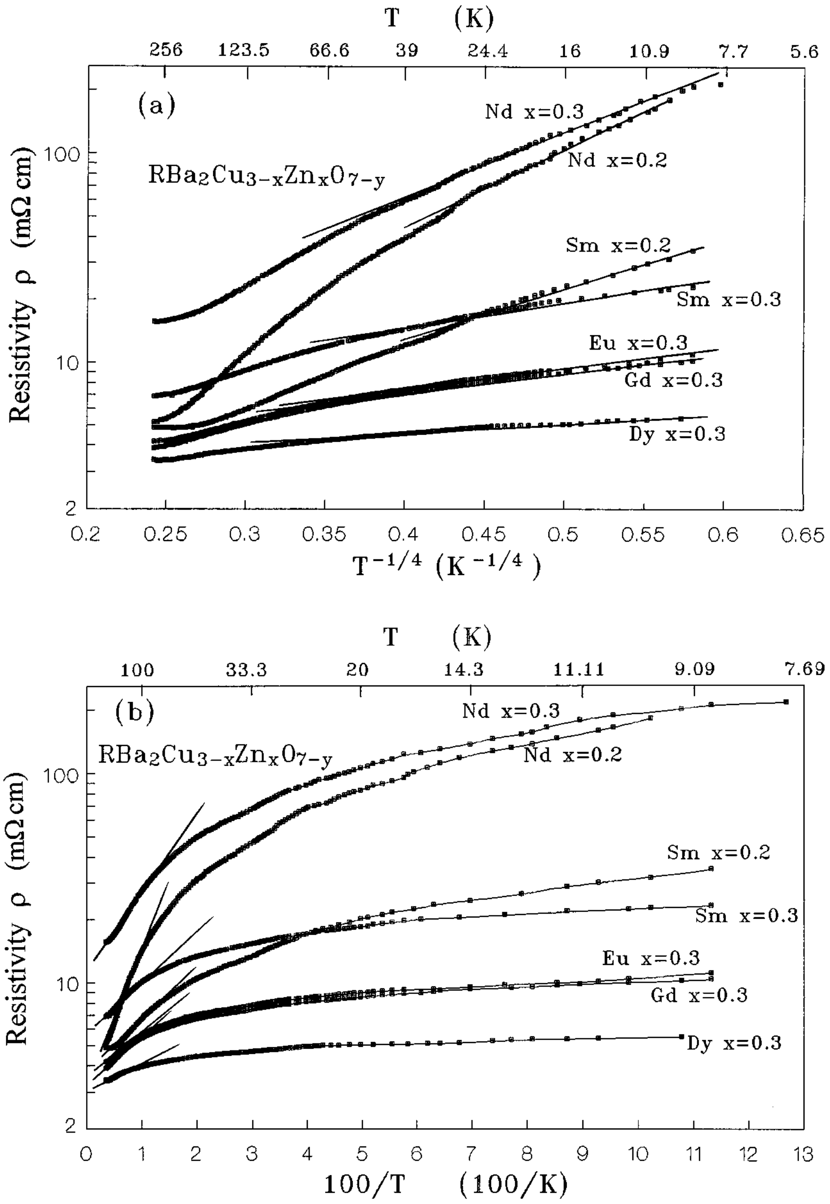

FIG. 4. Semilog plots of the resistivity ρ vs (a) $T^{-1/4}$ and (b) $100/T$ for $R\mathrm{Ba}_2\mathrm{Cu}_{3-x}\mathrm{Zn}_x\mathrm{O}_{7-y}$ (R=Dy, Gd, Eu, Sm, and Nd) with $x=0.2$ and 0.3.

tration $x=0.1$ either $T_{c,\,\mathrm{mag}}$ or the fraction of the magnetic shielding of the $\mathrm{RBa}_2\mathrm{Cu}_{2.9}\mathrm{Zn}_{0.1}\mathrm{O}_{7-y}$ samples is changed by varying the rare-earth element R. The samples with larger R ion radius have lower T_c and a small fraction of superconducting phase.

A plot of $T_{c,\mathrm{mid}}$ and $T_{c,\mathrm{mag}}$ versus ionic radius of the rare-earth elements R in $R\mathrm{Ba}_2\mathrm{Cu}_{3-x}\mathrm{Zn}_x\mathrm{O}_{7-y}$ (R=Yb, Er, Y, Dy, Gd, Eu, Sm, and Nd) is shown in Fig. 8. A closely linear relationship between T_c and the radius of R ions at low concentrations of Zn can be observed. At $x=0$ there is a slight increase in T_c on the R radius at low Zn concentration ($0.01<x<0.04$) can perhaps be attributed to the interplay between the tendencies of slightly increasing T_c with the radius at $x=0$ and slightly decreasing T_c with the radius at $x>0$. With rising Zn substitution ($x>0.06$), the suppression of T_c is apparently enhanced by increasing the ionic radius of the rare-earth elements R.

The effect of ion size on T_c for Zn-doped systems shown in Fig. 8 are similar to the observations in Pr-doped $R_{1-x}\mathrm{Pr}_x\mathrm{Ba}_2\mathrm{Cu}_3\mathrm{O}_{7-y}$ (R=Lu, Yb, Tm, Er, Ho, Y, Dy, Gd, Eu, Sm, and Nd) (Refs. 44–46) and in Ga-substituted $R\mathrm{Ba}_2\mathrm{Cu}_{3-x}\mathrm{Ga}_x\mathrm{O}_{7-y}$ (R=Yb, Er, Y, Dy, Ga, Eu, and Nd) (Refs. 47 and 48) systems. It should be noted, however, that this similarity between all Pr-, Ga-, and Zn-doped systems is only a formal resemblance, since Pr substitutes on R sites and the concentration of R is changed by introducing Pr, whereas Ga and Zn is replaced on the Cu(1) and Cu(2) sites, respectively, and the copper content is reduced by Ga- and Zn doping. For a specific RBCO system with different Pr-, Ga-, or Zn doping, the rates of T_c suppression dT_c/dx and the critical impurity concentration x_{cr} are different, implying different mechanisms for the degradation of superconductivity by various impurities.

Suppression of superconductivity by Zn doping has been intensively discussed.[1–43] Several suspected mechanisms for T_c suppression can be ruled out here: (1) There is no correlation between T_c and orthorhombic to tetragonal (O-T) transition, since orthorhombic structure is retained in 10% Zn-replaced RBCO systems. Shimizu, Kiyama, and Arai[42] observed that the O-T transition occurs only abruptly at up to

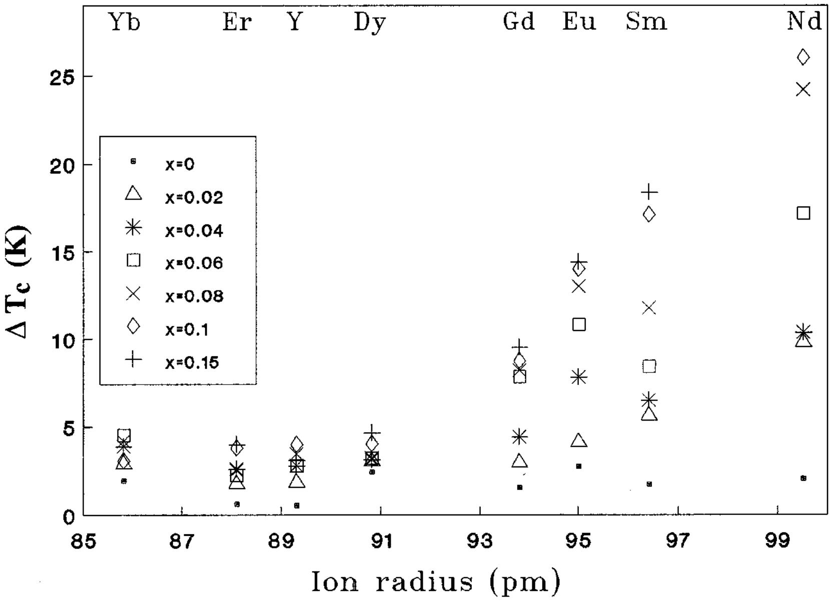

FIG. 5. The transition width ΔT_c, presenting the difference between $T_{c,\mathrm{mid}}$ and $T_{c,\mathrm{zero}}$, vs the ionic radius of rare-earth element R at various Zn concentration x for $R\mathrm{Ba}_2\mathrm{Cu}_{3-x}\mathrm{Zn}_x\mathrm{O}_{7-y}$ systems.

13% Zn-substituted GdBCO. (2) Because the oxygen stoichiometry remains nearly unchanged in 10% Zn-doped YBCO (Refs. 4, 11–13, 17, 23, and 25) and 16% Zn-doped GdBCO (Ref. 42) systems, the reduction of T_c is not caused by oxygen deficiency. (3) Due to the nonmagnetic nature of Zn ions the reduction of T_c by the magnetic moment of the dopant observed in Pr-doped systems[44] is unlikely. Walstedt *et al.*[29] estimated a moment-carrier exchange $J_{\mathrm{eff}}=20$ meV, which is more than an order of magnitude too small to account for the suppression of T_c in Zn-doped YBCO via Abrikosov-Gorkov pair breaking. They suggested an alternative explanation of pair breaking by strong potential scattering from the Zn impurity sites that requires d-wave pairing.[29]

The results of T_c depression due to Zn substitution can possibly be ascribed to the effect of disorder or a reduction in the carrier concentration. The magnetic penetration depth $\lambda(T)$ measurements were carried out on Zn-doped YBCO films by Ulm *et al.*,[58] and on magnetically aligned powders by Porch *et al.*[41] Both Refs. 58 and 41 show that Zn doping shows a particularly strong increase in $\lambda(0)$, implying that disorder results in the decrease of superconducting density of states, since in the London framework the increase in $\lambda(0)$ corresponds to a fourfold decrease in the number density of superconducting carriers: $n_s(0)\propto\lambda^{-2}(0)$. The substitution of Zn^{2+} (having a closed shell $3d^{10}$) for Cu possibly reduces the Cu $3d$ hole or slightly changes the state of hybridization between Cu $3d$ and O $2p$, thus decreasing the density of states at Fermi energy $N(E_F)$. Since Zn ions are in the same valence state as Cu^{2+}, Zn will not alter the charge balance within the CuO_2 plane, but would severely disorder and disturb the alignment of $\mathrm{Cu}(3d_{x2-y2})$ and $\mathrm{O}(2p_\sigma)$ orbitals, which would result in carrier localization in the CuO_2 planes. The localization effect arising from Zn substitution

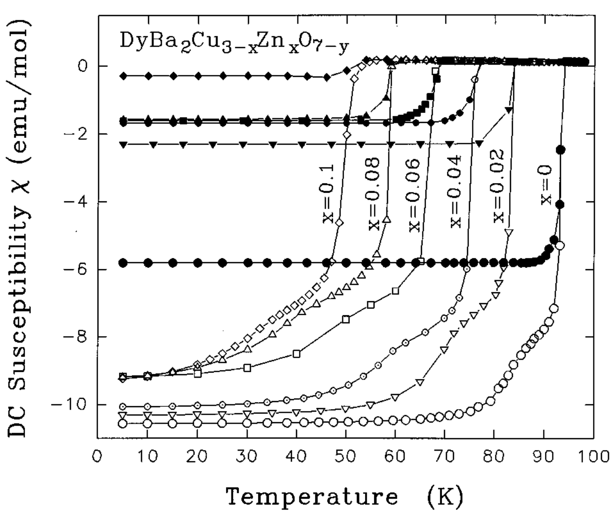

FIG. 6. dc susceptibility per mol χ of $\mathrm{DyBa}_2\mathrm{Cu}_{3-x}\mathrm{Zn}_x\mathrm{O}_{7-y}$ ($x=0$, 0.02, 0.04, 0.06, 0.08, and 0.1) vs temperature at both ZFC (open symbols) and FC (filled symbols).

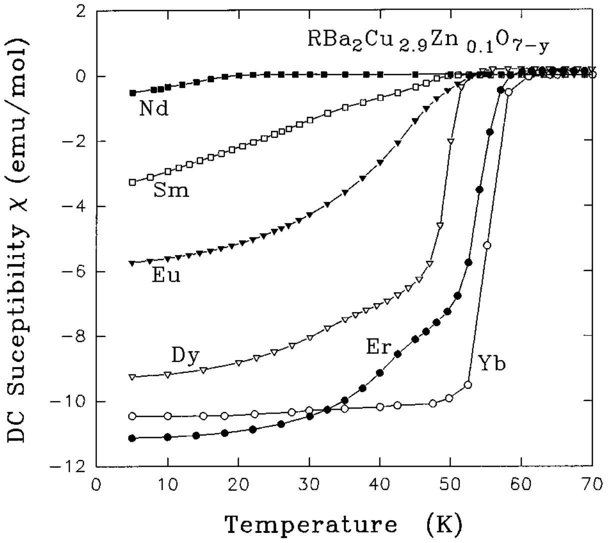

FIG. 7. A comparison of dc susceptibility per mol χ vs temperature for $R\mathrm{Ba}_2\mathrm{Cu}_{2.9}\mathrm{Zn}_{0.1}\mathrm{O}_{7-y}$ (R=Yb, Er, Dy, Gd, Eu, Sm, and Nd).

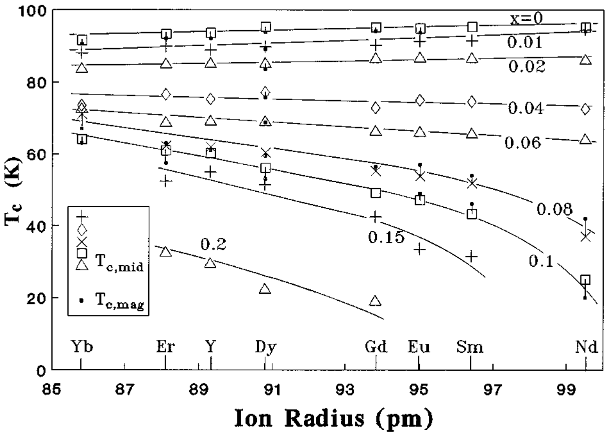

FIG. 8. A plot of the superconducting transition temperature T_c [(+□△◇×) represent $T_{c,\mathrm{mid}}$ at various values of x, and (▪) represents $T_{c,\mathrm{mag}}$] for $R\mathrm{Ba}_2\mathrm{Cu}_{3-x}\mathrm{Zn}_x\mathrm{O}_{7-y}$ against the ionic radius of the rare-earth element R at different Zn concentrations.

can then account for the metal-semiconductor transition and thus the destruction of superconductivity.

The ion size effect was established for Pr-doped (on Y sites) systems,[44–46] and also found for Ga-doped [on the Cu(1) sites in Cu-O chains] systems.[47,48] In the present work we find that this R ionic size effect also exists in Zn-doped [on the Cu(2) sites in Cu-O$_2$ planes] $R\mathrm{Ba}_2\mathrm{Cu}_{3-x}\mathrm{Zn}_x\mathrm{O}_{7-y}$ systems. Although the mechanism of the rare-earth ion size effect on T_c and ρ by Zn doping is not well understood yet, we propose a possible interpretation in terms of Mott's spin-bipolaron model.[31,59]

Mott[31,59] supposes that in the copper oxide p-type superconductors the carriers (O $2p$ holes) form bipolarons (bosons) above and below T_c. The spin on an oxygen hole is locked antiparallel to one of the Cu $3d^9$ spins. Two of these polarons form a bipolaron (boson) of zero moment with a binding energy of ~ 0.3 eV. The motion of bipolarons is diffusive, activated by spin flip. In the superconducting state the holes form a degenerate gas of bosons, interacting but not strongly overlapping as do the BCS pairs. At $T \geqslant T_c$ the Bose gas becomes nondegenerate (above T_c the current is carried by a nondegenerate gas of bosons). The bosons are in an impurity band, so that boson states up to a limiting energy E_c are Anderson localized. On account of the strong repulsion between the bosons, Mott proposes that not more than one boson can be in a given state, even above the mobility edge. The energy up to which states are singly occupied, behaving like a Fermi energy, is named E_B (or pseudo-Fermi-energy $E_{F'}$). If E_B lies in the range of localized states, the material cannot be a superconductor, and the bosons cannot move. Only if E_B lies above E_c will a superconductor form. If states are still localized, the conduction should be due to variable range hopping. This model was used to interpret experimental observations on copper oxide superconductors: the constant value of specific heat over temperature, C_V/T,[30] the small entropy at superconducting transition (much smaller than $Nk\ln 2$), the linear dependence of resistivity on temperature (above T_c, $\rho \propto T$), the Hall effect, the thermopower, the observed Fermi surface, and so on.[31,59]

For Zn-doped YBCO, Mott supposes that the effect of zinc, which produces disorder in the planes, is to prevent pairing and to render the polarons immobile (Anderson localization). The presence of zinc will result in an increase in the mobility edge E_c, moving it up eventually to E_B, destroying the superconductivity.

In our case for an insulating compound $R\mathrm{Ba}_2\mathrm{Cu}_{3-x}\mathrm{Zn}_x\mathrm{O}_{7-y}$, where x is large enough to suppress T_c to zero, the pseudo-Fermi-energy E_B is lower than E_c. A transition of the Anderson type of metallic behavior should occur when E_B crosses the mobility edge as the content of zinc is reduced. As $x < x_{\mathrm{cr}}$, the bosons above the mobility edge produce the superconductivity. The rare-earth ion size effect on T_c of $R\mathrm{Ba}_2\mathrm{Cu}_{3-x}\mathrm{Zn}_x\mathrm{O}_{7-y}$ observed in this work could then be ascribed to the ion size effect on E_c and/or E_B at constant x. This means that for the same amount of zinc replacing copper, the range of localized states is affected by the R plane. An increase in the ionic size of R will move the mobility edge E_c upwards and/or will lower E_B in $R\mathrm{Ba}_2\mathrm{Cu}_{3-x}\mathrm{Zn}_x\mathrm{O}_{7-y}$ systems.

In conclusion, we have systematically studied the effect of Zn doping on the resistivity ρ, dc susceptibility χ, and superconducting T_c of $R\mathrm{Ba}_2\mathrm{Cu}_{3-x}\mathrm{Zn}_x\mathrm{O}_{7-y}$ systems (R=Yb, Er, Y, Dy, Gd, Eu, Sm, and Nd, and $0 \leqslant x \leqslant 0.3$). We have found that (1) Zn atoms substitute more likely on the Cu(2) sites, (2) Zn doping in these systems causes a rapid nearly linear decrease in T_c as Zn content increases, and (3) the reduction of T_c for $R\mathrm{Ba}_2\mathrm{Cu}_{3-x}\mathrm{Zn}_x\mathrm{O}_{7-y}$ depends on the ionic radius of the rare-earth element R. The suppression of superconductivity by zinc and the rare-earth ion size effect on T_c in these systems is interpreted in terms of a Mott spin bipolaron model.

ACKNOWLEDGMENTS

We wish to thank Professor A. Braginski for the support, the suggestion of Raman measurements and discussions, Professor H. Lüth for support, Professor Weiyan Guan, Professor Ch. Heiden, and Dr. H. Münder for discussions, and Dr. C. Freiburg and W. Reichert for experimental help.

---

*Present address: Institut Für Angewandte Physik, Universität Gießen, Heinrich-Buff-Ring 16, 35392 Gießen, Germany.

†Present address: Reactor and Neutron Physics Department, Nuclear Research Center, AEA, Cairo, Egypt.

[1] G. Xiao, M. Z. Cieplak, A. Garvrin, F. H. Streitz A. Bakhshai, and C. L. Chien, Phys. Rev. Lett. **60**, 1446, (1988); G. Xiao *et al.*, Nature **332**, 238 (1988); Phys. Rev. B **35**, 8782 (1987).

[2] Y. Maeno, T. Tomita, M. Kyogoku, S. Awaji, Y. Aoki, K. Hoshino, A. Minami, and T. Fujita, Nature **328**, 512 (1987).

[3] Youwen Xu, R. L. Sabatini, A. R. Moodenbaugh, and M. Suenaga, Phys. Rev. B **38**, 7084 (1988); Y. Xu *et al.*, *ibid.* **39**, 6667 (1989); Physica C **169**, 205 (1990).

[4] J. M. Tarascon, P. Barboux, P. F. Miceli, L. H. Greene, G. W. Hull, M. Eibschutz, and S. A. Sunshine, Phys. Rev. B **37**, 7458 (1988); J. M. Tarascon *et al.*, *ibid.* **36**, 8393 (1987); P. F. Miceli *et al.*, *ibid.* **37**, 5932 (1988).

[5] M. Mehbod, W. Biberacher, A. G. M. Jansen, P. Wyder, R. Deltour, and P. H. Duvigneaud, Phys. Rev. B **38**, 11 813 (1988); M.

Mehbod *et al.*, *ibid.* **36**, 8819 (1987).

[6] H. Maeda, A. Koizumi, N. Bamba, E. Takayama-Muromachi, F. Izumi, H. Asano, K. Shimizu, H. Moriwaku, H. Maruyama, Y. Kuroda, and H. Yamazaki, Physica C **157**, 483 (1989).

[7] N. W. Shafer, T. Penney, B. L. Olson, R. L. Greene, and R. H. Koch, Phys. Rev. B **39**, 2914 (1989).

[8] T. J. Kistenmacher, Phys. Rev. B **38**, 8862 (1988).

[9] H. Alloul, T. Ohno, H. Casalta, J. F. Marucco, P. Mendels, J. Arabski, G. Collin, and M. Mehbod, Physica C **171**, 419 (1990); P. Mendels, H. Alloul, J. F. Marucco, J. Arabski, and G. Collin, *ibid.* **171**, 429 (1990).

[10] R. Dupree, A. Gencten, and D. McK.Paul, Physica C **193**, 81 (1992); A. Gencten, R. Dupree, and D. McK.Paul, *ibid.* **216**, 491 (1993).

[11] R. Liang, T. Nakamura, H. Kawaji, M. Itoh, and T. Nakamura, Physica C **170**, 307 (1990).

[12] C. S. Jee, D. Nichols, A. Kebede, S. Rahman, J. E. Crow, A. M. Ponte Goncalves, T. Mihalisin, G. H. Meyer, I. Perez, R. E. Salomon, P. Schlottmann, S. H. Bloom, M. V. Kuric, Y. S. Yao, and R. P. Guertin, J. Supercond. **1**, 63 (1988).

[13] C. L.-Gledel, J.-F. Marucco, B. Touzelin, R. Gabilly, A.P.-Philippot, and H. Alloul, Physica C **172**, 304 (1990).

[14] Y. Shimakawa, Y. Kubo, K. Utsumi, Y. Takeda, and M. Takano, Jpn. J. Appl. Phys. **27**, L1071 (1988).

[15] T. Kajitani, K. Kusaba, M. Kikuchi, Y. Syono, and M. Hirabayshi, Jpn. J. Appl. Phys. **27**, L354 (1988).

[16] E. Takayama-Muromachi, Y. Uchida, and K. Kato, Jpn. J. Appl. Phys. **26**, L2087 (1987).

[17] K. Westerholt, H. J. Wüller, H. Bach, and P. Stauche, Phys. Rev. B **39**, 11 680 (1989).

[18] B. Roughani, L. C. Sengupta, J. L. Aubel, S. Sundaram, and W. C. H. Joiner, Physica C **171**, 77 (1990).

[19] B. Jayaram, S. K. Agarwal, C. V. Narasimha Rao, and A. V. Narlikar, Phys. Rev. B **38**, 2903 (1988).

[20] G. Balakrishnan, L. W. J. Caves, R. Dupree, D. McK. Paul, and T. Smith, Physica C **161**, 9 (1989).

[21] C. Y. Yang, A. R. Moodenbaugh, Y. L. Wang, Y. W. Xu, S. M. Heald, D. O. Welch, M. Suenaga, D. A. Fischer, and J. E. Pennerhahn, Phys. Rev. B **42**, 2231 (1990).

[22] H. Yamagata, K. Indana, and M. Matsumura, Physica C **185-189**, 1101 (1991).

[23] J. L. G-Munoz, X. Obradors, S. H. Kilcoyne, and R. Cywinski, Physica C **185-189**, 1085 (1991).

[24] G. Roth *et al.*, Physica C **162-164**, 518 (1989).

[25] A. Lanckbeen, C. Legros, J. F. Marucco, and R. Deltour, Physica C **221**, 53 (1994).

[26] Pan Wei and Zheng Qing Qi, Physica C **183**, 32 (1991).

[27] R. S. Howland *et al.*, Phys. Rev. B **39**, 9017 (1989).

[28] X. Zhang, K. W. Yip, and C. K. Ong, Physica C **234**, 99 (1994).

[29] R. E. Walstedt, R. F. Bell, L. F. Schneemeyer, J. V. Waszczak, W. W. Warren, Jr., R. Dupree, and A. Gencten, Phys. Rev. B **48**, 10 646 (1993).

[30] J. W. Loram, K. A. Mirza, and P. F. Freeman, Physica C **171**, 243 (1990).

[31] N. F. Mott, Physica C **196**, 369 (1992).

[32] Y. Nakazawa, J. Takeya, and M. Ishikawa, Physica C **174**, 155 (1991).

[33] J. T. Kim, T. R. Lemberger, S. R. Foltyn, and X. D. Wu, Phys. Rev. B **49**, 15 970 (1994).

[34] T. R. Chien, Z. Z. Wang, and N. P. Ong, Phys. Rev. Lett. **67**, 2088 (1991).

[35] V. Radhakrishnan *et al.*, Phys. Rev. B **40**, 6850 (1989).

[36] M. Affronte *et al.*, Solid State Commun. **70**, 951 (1989).

[37] A. I. Akimenko, G. Goll, H.v. Löhneysen, and V. A. Gudimenko, Physica C **213**, 399 (1993).

[38] H. Harashina *et al.*, Physica C **212**, 142 (1993).

[39] P. Stropel, C. Paulsen, and J. L. Tholence, Solid State Commun. **65**, 585 (1988).

[40] J. A. Hodges *et al.*, Physica C **218**, 272 (1993).

[41] A. Porch *et al.*, Physica C **214**, 350 (1993).

[42] H. Shimizu, T. Kiyama, and J. Arai, Physica C **196**, 329 (1992).

[43] S. S. Ata-Allah, Yunhui Xu, and Ch. Heiden, Physica C **221**, 39 (1994).

[44] Yunhui Xu and Weiyan Guan, Phys. Rev. B **45**, 3176 (1992); Solid State Commun. **80**, 105 (1991); Physica C **183**, 105 (1991); Appl. Phys. Lett. **59**, 2183 (1991); Phys. Lett. A **163**, 104 (1992); Physica C **199**, 430 (1992).

[45] W. Y. Guan, Y. C. Chen, J. Y. T. Wei, Y. H. Xu, and M. K. Wu, Physica C **209**, 19 (1993).

[46] W. Y. Guan, Y. H. Xu, S. R. Sheen, Y. C. Chen, J. Y. T. Wei, H. F. Lai, M. K. Wu, and J. C. Ho, Phys. Rev. B **49**, 15 993 (1994).

[47] Yunhui Xu and Weiyan Guan, Physica C **212**, 119 (1993).

[48] Yunhui Xu, Weiyan Guan, Y. F. Chen, S. R. Sheen, and M. K. Wu, Phys. Rev. B **50**, 1223 (1994).

[49] F. E. Bates, Phys. Rev. B **39**, 322 (1989); F. E. Bates and J. E. Eldridge, Solid State Commun. **64**, 1435 (1987).

[50] R. Feile, Physica C **159**, 1 (1989).

[51] C. Thomsen and M. Cardona, in *Physical Properties of High Temperature Superconductors I*, edited by D. M. Ginsberg (World Scientific, Singapore, 1988), pp. 409-507.

[52] L. C. Sengupta *et al.*, Physica C **165**, 125 (1990).

[53] A. Erle and G. Güntherodt, Physica C **171**, 216 (1990).

[54] E. Sodtke, C. Andrzejak, D. Guggi, and Y. Xu, Physica C **180**, 50 (1991).

[55] N. F. Mott, J. Non-Cryst. Solids **1**, 1 (1968); N. F. Mott and E. A. Davis, *Electronic Processes in Noncrystalline Materials*, 2nd ed. (Clarendon, Oxford, 1979).

[56] B. I. Shklovskii and A. L. Efros, *Electronic Properties of Doped Semiconductors*, Springer Series in Solid-State Sciences Vol. 45 (Springer-Verlag, Berlin, 1984), pp. 26–30 and 76.

[57] Yunhui Xu and Weiyan Guan, Physica C **206**, 59 (1993).

[58] E. R. Ulm, J. T. Kim, T. R. Lemberger, S. R. Foltyn, and X. Wu, Phys. Rev. B **51**, 9193 (1995).

[59] N. F. Mott, Adv. Phys. **39**, 55 (1990); Philos. Mag. Lett. **62**, 37 (1990); **63**, 319 (1991); **64**, 211 (1991); **64**, 411 (1991).